Getting the Best out of PRESTO - Part 3: Waterfalls and Conclusions

Peter East

Abstract

This article completes an investigation into replacing the Chi-square statistic with the peak SNR (signal-to-noise ratio) measure in the PRESTO *prepfold* processes; in this case, to the waterfall graphic [1,2]. With this small change, improved recognition confidence is possible for lower SNR intercepts. Better target visibility is achieved by reducing the number of waterfall time sections and/or applying an accumulating folding algorithm. Finally, a complete low SNR comparison *prepfold* plot is offered based on the information in all three articles. A MathCad program duplicating the *prepfold* processes to produce this completed plot is presented in Appendix 2. Some additional pulsar recognition/confirmation features are also described.

Introduction

The PRESTO *prepfold* software tool rapidly carries out a number of processes on a data file and outputs a graphical plot as shown in Figure 1 [3,4]. The various processes normally combine to provide sufficient information for an operator to confidently confirm the acquisition of a real pulsar; except if, as in this case, the pulsar signal-to-noise ratio (SNR) is below about $\sqrt{\sqrt{2}P/W}$:1 (where P is the pulsar period and W the half-height pulse width - in the same units).

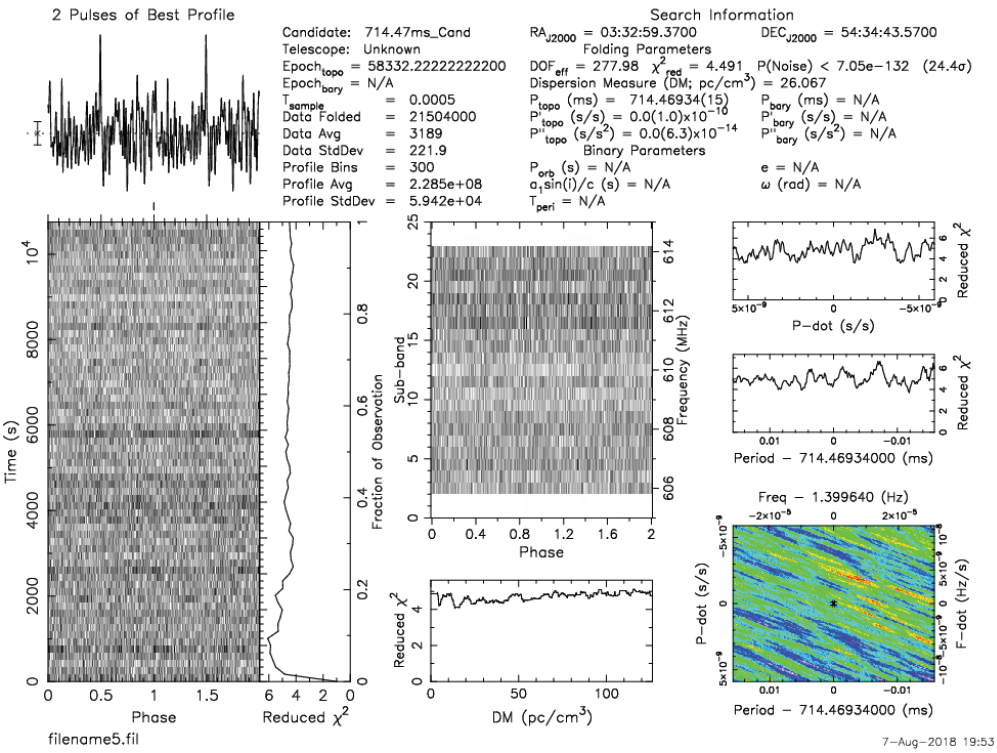

Figure 1. Typical 5:1 SNR Example PRESTO *prepfold* plot using the Chi-square amplitude statistic.

The sub-plots and normal recognition features identified, are summarized below,

1. Pulse profile plot (located top-left of PRESTO plot)

   Pulse profile and amplitude on folded noise base - two periods shown to improve visibility at phase extremities.

2. Waterfall and Reduced-Chi-square running value plots (located left side).

   For large SNRs, vertical dark lines or vestiges directly below the pulse profile plot (none visible here) with possible dropouts indicate the intercept of a regular, but scintillating pulse train. Not always clear for even quite large SNRs. Most *prepfold* runs appear to split the data into 64 sections, effectively reducing the observed SNR by a factor of 8, which may limit the pulse train visibility. The Reduced Chi-

square section to the right of the waterfall should indicate a cumulative growth of the statistic from a starting value of one and then to exhibit a continuous, mainly rising, amplitude trend. In this case, there appears an anomalous offset at the beginning and no evidence of the measure growth.

3. Frequency sub-band plot - (located in center).
   Again for large SNRs semi-continuous vertical lines consistent with the pulse profile phase position (again, not visible here) indicating scintillating frequency components in all sub-bands as expected from the broad-band nature of pulsar signals.
4. Dispersion Measure sub-plot - (located center bottom).
   A peak is expected at the known dispersion measure (DM) of the pulsar source (not visible here) implying that the signal is extra-terrestrial and typical of traveling a distance through interstellar space. Note that all other plots require the data to be correctly de-dispersed.
5. P-dot, period search and correlated p-dot/period search plots - right-hand side.
   Peaks are expected at zero search error in all three plots. Also, a peak (red) elliptical feature is expected at zero error in the p-dot/period graphics plot; signifying expected accurate pulsar period with negligible frequency or period rate drift. The ellipse is normally extended and slope should equate to -2/N, where N is the number of pulsar periods in the data sample.

** Note on Chi-square interpretation: The reduced chi-square statistic value should increase with both pulse amplitude and duty cycle and be equal to unity for pure Gaussian noise. RFI that impacts the Gaussian distribution will increase the statistic value and tend to obscure any pulsar present until the pulsar SNR becomes significant. This situation is clear in the Figure 1. running Chi-square plot beside the waterfall. The reduced Chi-square value immediately rises to between 5 and 6 indicating significant non-Gaussian initial offset and further, the pulsar signal present fails to overcome this throughout the data duration. When judging the effectiveness of DM, period and p-dot search plots, the effect of residual noise distortion is to reduce the statistic discrimination.*

Positive evidence in all five cases (seven plots) builds the required recognition confidence (see Table 1.). Normally, depending on the pulsar duty cycle, intercept SNRs well above 12:1 (for 1% duty cycle) are required. The 5:1 SNR example in Figure 1, shows that at this SNR level, apart from the pulse profile, the other sub-plots provide no positive recognition information at all.

Earlier articles have indicated the data peak SNR statistic improves the majority of these sub-plots. The present article applies peak data SNR tracking to point 2. above; the waterfall and associated confidence plots.

Amateurs have been satisfied with just a large value SNR result and in some cases correct period and DM search peaks. It is known however that in modest to low SNR cases, that this is insufficient and that other pulsar properties may need to be evaluated to improve analysis confidence.

There is now a trend for amateurs to require this evidence only from professional software which may not have been intended for this task. This third article offers a considered response to this criterion by showing that by duplicating PRESTO algorithms but applying the peak SNR measure, pulsar validation confidence can be extended to much lower target SNRs.

PRESTO Recognition Summary

Table 1 Checks on Essential Pulsar Properties

Sub-plot	**Property**
Profile	pulse shape/width
Time Waterfall/cumulative plot	scintillating pulse train
Frequency Waterfall	scintillating wide band noise
DM Plot	correctly dispersed - interstellar source
Period Search	accurate matched period
P-dot Search	negligible spin-down
Period/P-dot Plot	high stability pulse train

Positive indications in the Table 1 sub-plots confirms the presence and matching of the listed pulsar properties. All should be satisfied for sufficient evidence to prove a correct intercept.

The Final Folded Pulsar Profile

Figure 2 shows the final folded result of 10,000 periods producing modest SNR with the data bandwidth reduced to pass the expected pulse profile [5].

All large transient spike RFI and other RFI spectral harmonics have been blanked. The central candidate is obvious but the varying folded noise base has very similar characteristics and there is a small chance that the central peak could also be an unusual noise peak. This conclusion becomes more likely in cases where the integrated peak is lower.

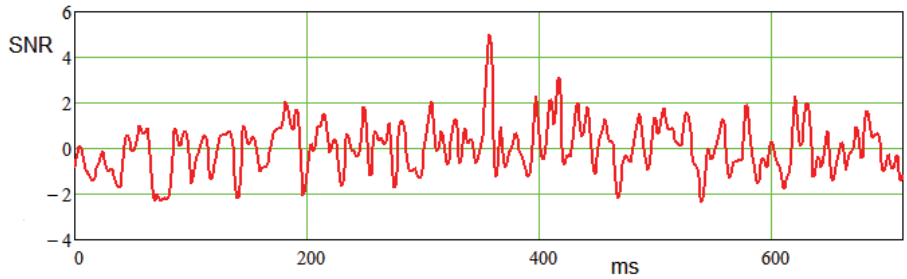

Figure 2. 5:1 SNR B0329+54 Example Matched-Period Fold of 10000 Periods.

This particular plot is the result of integrating some 150 billion samples of data down to just 714 points and whilst it is acknowledged that the folding algorithm is the optimum for maximizing the best signal-to-noise ratio, other valuable validation information may still reside in the recorded data. A relevant sub-fold correlation method to minimize noise ambiguities and highlight strong candidates is discussed later.

Spectral recognition methods are not viable at this low SNR level as, once folded, the noise occupies and obscures the same harmonic line structure as the wanted pulsar spectrum. The pulse bandwidth-limited fold algorithm provides the best pulsar SNR possible.

The Waterfall Plot

Figure 3 shows a 'waterfall' plot (flowing upwards). For this plot the data file of Figure 2 was divided into four equal sections and folded separately before combining in the contour graphic (red strong positive, blue strong negative). The central pulsar signal fills each section as expected but, as discussed above, some noise peaks remain present for two or more sections. When dividing into many more sections, the central pulsar feature reduces by the square root of the number of sections and eventually drops below the mean noise peaks noise and so to invisibility.

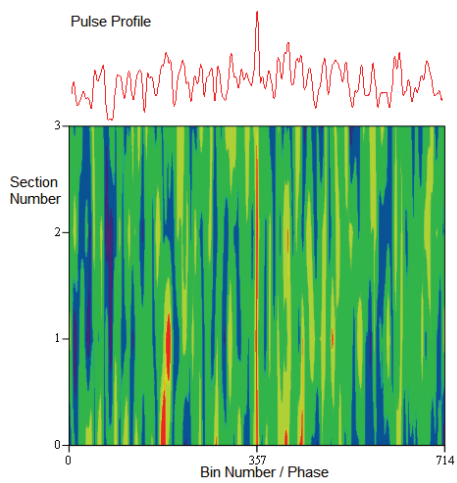

Figure 3. 5:1 SNR B0329+54 Example Matched-Period 4-Section Fold of 10,000 Periods.

In this example the Figure 2 pulsar peak SNR is reduced by one half (1/√4 for four sections).

It is this reduction in component SNR with increased waterfall sections that is responsible for the poor visibility of pulsar presence in the Figure 1 time-waterfall plot. In general, for a waterfall plot, a reasonable

goal is to limit the number of sections '*S*' so that the section expected SNR does not drop much below 2.5:1; with this proposed constraint the candidate integrated fold SNR should be greater than $2.5\sqrt{S}$.

Cumulative SNR Plot (Analysis and Software in Appendix 2)

This section investigates using the cumulative SNR measure instead of the *prepfold* cumulative Chi-square statistic. For this plot, the data is again divided into a number of equal sections (now 100), each section is folded, but in this case, the sections are accumulated sequentially before folding and the SNRs calculated for the increasing section sums and plotted.

In Figure 4, the brown plot follows the cumulative peak SNR; this may report either the maximum noise peak or, if significant, any pulsar pulse amplitude whichever is largest. It also shows the central bin pulsar candidate's SNR (red); which appears to increase roughly as the square root of the number of sections, as is predicted. The variations may also be expected due to base noise, source scintillation and/or random effects of residual RFI features along the data record. The red curve shows that the pulsar candidate takes over from random noise peaks as the accumulated SNR exceeds about 3:1. This is a powerful tool for not only differentiating pulsar candidates and noise, but to recognize the impact of scintillation and/or sporadic RFI; ignoring/removing these sections can improve the final pulsar SNR (see Appendix 1).

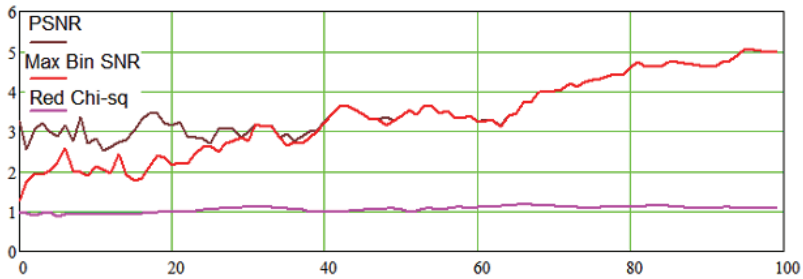

Figure 4. 5:1 SNR B0329+54 Example Accumulated Section SNR

The presence of scintillation means that the cumulative integration pattern will be different depending on whether the integration is carried out from beginning to end or, from end to beginning. The end results of both will always be the same but the path to get there will be different and hint at the stronger scintillation regions. For completeness in Figure 4, the Chi-square cumulative statistic is calculated for the data and plotted in magenta. As discussed in earlier articles it starts with a value of 1 indicating the base noise is closely Gaussian/Normal and rises very little being relatively insensitive to the low-level, low duty cycle pulsar candidate and non-presence of significant RFI (see Reference 1).

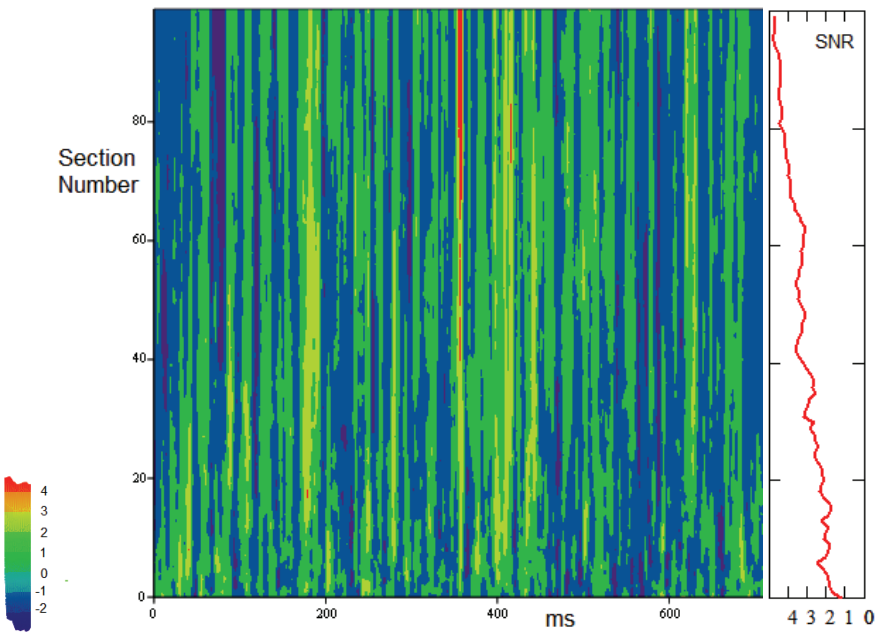

Figure 5. 5:1 SNR B0329+54 Example Accumulated SNR Waterfall

A more instructive PRESTO comparison approach is to plot this accumulated SNR as a waterfall plot showing all the data as in Figure 5. In this method, instead of displaying a few sub-section fold results, a larger number of accumulating folds, such that by the final section, the sum fold of all the data is presented.

Figure 5 shows much more clearly the suppression of random noise components and the final dominance of this low SNR pulsar candidate's response (red). There are some drop-outs of the integrating signal possibly indicating the effects of scintillation, but the final pulsar line width is in keeping with its pulse width/period ratio. The vertical lower-level noise features (green bands) show that the final noise peaks appear present throughout the record but tend not to integrate as does the true pulse train; This appears a memory effect, not evident in the standard time section waterfall of Figure 3; once a strong peak section is accumulated, it appears to take many sections to get washed out and is susceptible to being re-invigorated by subsequent section peaks. Expected randomness only appears in the initial 5-10 sections. It is not obvious why this occurs but it appears due to the fine harmonic frequency filtering property of the folding algorithm.

Combined Data Comparison Plot

Combining the information discussed above with the results of the earlier articles, it is now possible to compare the results of using SNR rather than Chi-square to sense the pulsar presence [1,2].

Figure 6 shows the PRESTO *prepfold* SNR look-alike plot. An extra inclusion is the frequency spectrum (center) plot; the data used was recorded using a 3-band RTL receiver, each of 2 MHz bandwidth centered on 609, 611, and 613 MHz [5]. The detailed MathCad data analysis and algorithms are given in Appendix 2.

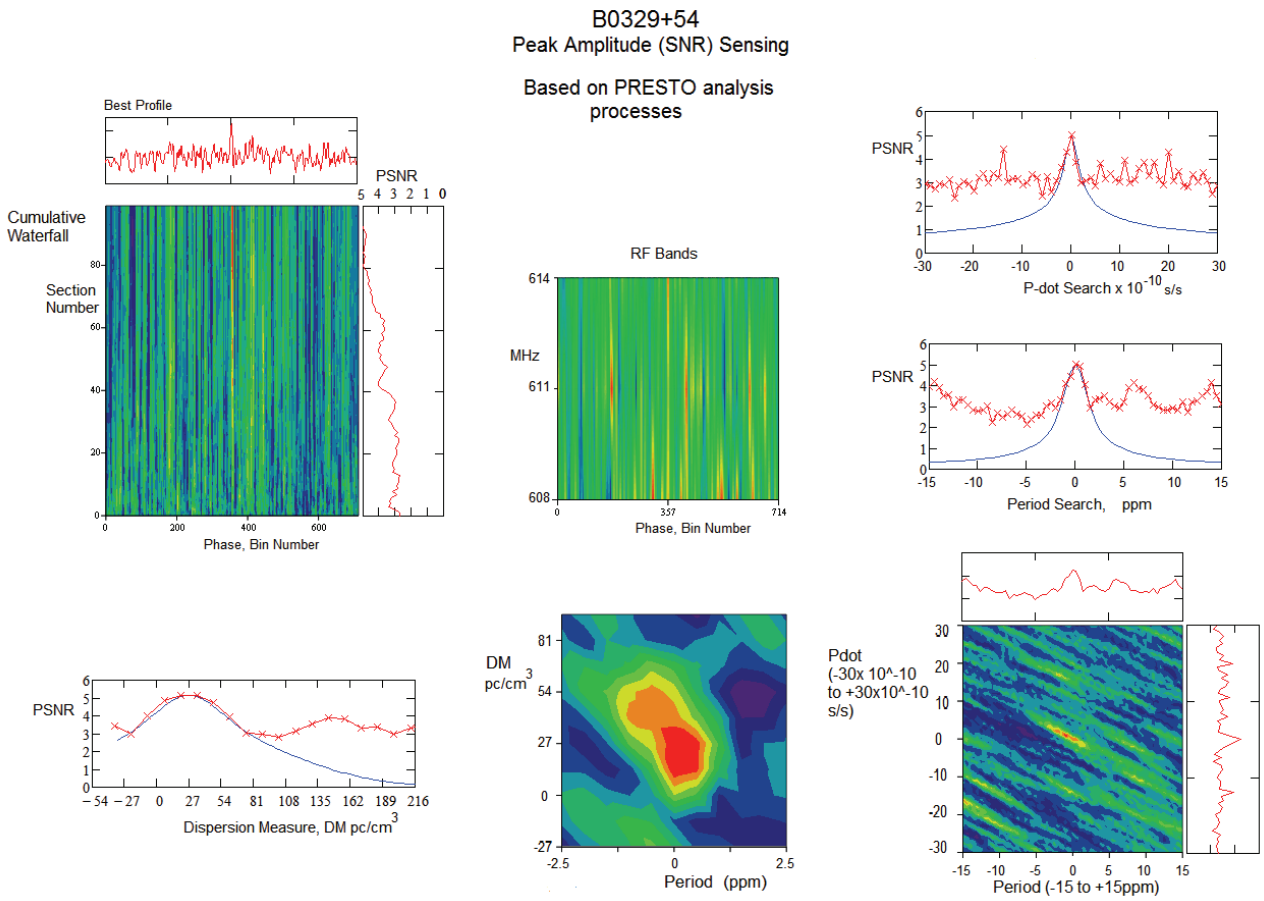

Figure 6. 5:1 SNR B0329+54 Example PRESTO *prepfold* Comparison Plot

Comparing Figure 6 with the 5:1 SNR *prepfold* plot in Figure 1 it is concluded that all PRESTO-approved pulsar recognition features are now clearly evident; just by using the maximum SNR rather than the Chi-square statistic. To improve clarity, the *prepfold* time waterfall plot has been replaced with the accumulated 100-section waterfall. For the DM, period search and p-dot search plots, the blue curves

included are those calculated for an ideal noise-less pulse train matching the pulse characteristics of the target pulsar [6]. The calculated curves have been normalized to the measured data peaks and in the case of the DM plot, the peak was adjusted by half the data sample time; again to match peaks and to accommodate the data timing coarseness. The close match of data and theory is an additional strong indicator of the pulse train-like characteristic of the candidate pulsar. Included for interest, as it is offered in other professional software, is the 2-D DM/Period plot showing maximum correlation about DM=27 and zero period error. It should be admitted that there was a large time penalty to obtain the detail of Figure 6; the plots were assembled manually from MathCad for this exercise but it would seriously benefit from the power of a Python GUI!

Noise Rejection by Cross-Correlation

Pulsar identification information used by PRESTO, listed in Table 1, looks only at the essential pulsar parameters. The parameter search routines described in Reference 6 utilize more detailed search prediction features to add weight to pulsar recognition; specifically, calculated changes in bin position and pulse width. The time and frequency waterfalls can confirm an extensive pulse train and a broadband source with scintillation present in both parameters. In all, this represents convincing evidence of a true pulsar acquisition. All of these techniques exploit the pulse-train-like and intrinsic properties of pulsars. Three other techniques have been investigated that exploit noise properties throughout the recorded data to add weight to the recognition process especially at very low SNR levels; these are the cumulative SNR plot described in this paper, the multi-bin folding algorithm extension evaluated in Reference 8, and the half-fold multi-correlation procedure described in Reference 7. This is by no means the end of the list of anticipated features that add recognition confidence; there is the simple check in drift-scan mode, for increased level and density of pulsar data on the antenna boresight for example.

A demonstration of multi-fold correlation using the data file of Figure 6 is shown in Figure 7.

In the upper part of Figure 7 is shown the overlaid results of the example data file divided into 8 sections which are individually folded. It is clear from this that the central section containing the pulsar candidate (separated and magnified to the right) exhibits variable, but positive co-located peaks (ranging from 0.8:1 SNR to 2.8:1 SNR). The remaining 'noise' components appearing random. Summing these section results, with suitable scaling, produces the expected all-data fold appearing in red in the lower plot.

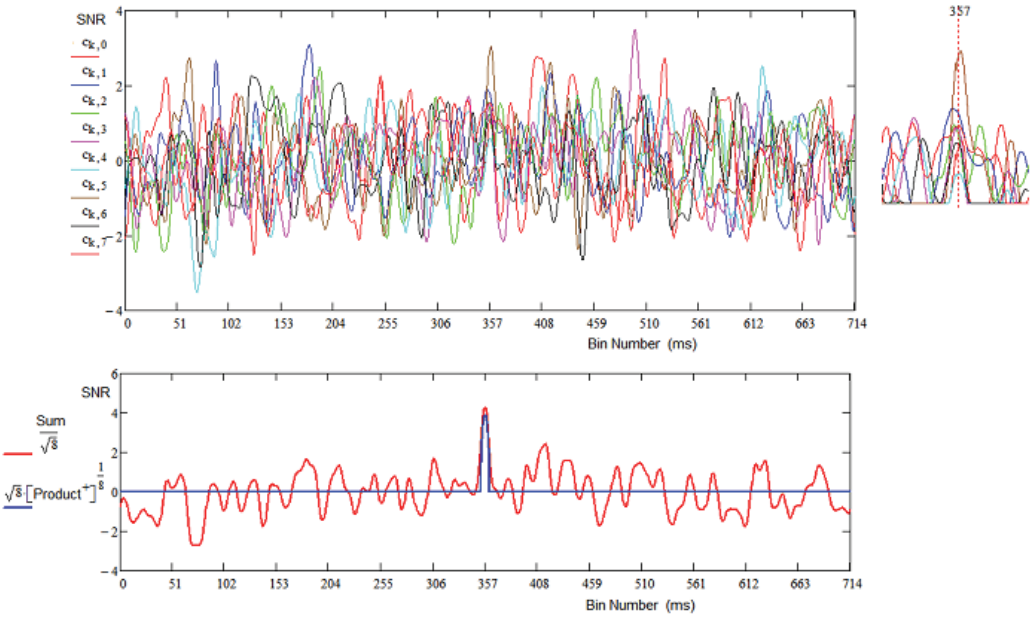

Figure 7. 8-Section Data Correlation

The correlation algorithm multiples the positive folded excursions together and in this case, takes the eighth root and factors as indicated on the left side of the lower plot to produce the blue curve shown. This algorithm appears to zero the noise but pass the regular pulse train pulsar shape with minimal amplitude reduction. Providing scintillation does not zero a section, this technique will always preferentially

display the pulsar pulse region. Experimentation, either with number of sections or combining randomized data half-folds may be necessary in general to fully zero all noise peaks [7]. It is considered that randomized data half fold combining would be somewhat more robust. The algorithm is an extension of the two variable near identity: $\sqrt{2\ a\ b} \approx (a+b)/\sqrt{2}$, unless *a* or *b* approach zero.

Conclusions

This is the latest article in a series studying the problem of recognizing and identifying a weak pulsar in recorded data collected by amateur radio telescopes. The key indicator and problem is the powerful epoch folding algorithm. This reduces gigabytes of collected data to a few hundred bytes, optimally matched to the wanted pulsar pulse width and repetition period. This maximizes the pulsar signal to noise ratio. For weak SNRs it is superior to any spectrum technique. However, the final fold signal and noise pattern is now fixed; noise frequency components occupy the same frequency harmonics as the wanted pulsar signal and all may be simply considered as pulsar-like signals of different phases.

The three articles have explored the benefit to amateurs of using the maximum SNR measure rather than the reduced Chi-square statistic as is used in the PRESTO *prepfold* pulsar processing tool. The benefit is much better visibility of low SNR pulsar acquisitions below 12:1 (1% pulse duty cycle). PRESTO uses the Chi-square statistic for good reasons; firstly it requires less computing power and hence much faster and secondly, the primary aim of PRESTO is to search for new pulsars of unknown pulse width, period and dispersion; it is very efficient at searching this wide triple-parameter range. Amateurs are unlikely to be in the same class for discovering new pulsars but will know the target parameters. They can optimize data processing bandwidths and may have more time on their hands for extracting pulsar-recognition detail.

The techniques described in these three articles duplicate the PRESTO *prepfold* tool processes and provide much more recognition information detail and can prove more useful for validating weak, but genuine, pulsar intercepts for either small or large antenna systems. In short, a straight comparison between Figures 1 and 6 shows that with this change, a much more amateur-friendly pulsar recognition plot results.

Postscript

Detection and recognition of the loudest pulsars is definitely within the capability of all amateurs with modest but well-designed and tuned antenna/receiver systems; certainly in drift-scan observation mode. There may be problems, however, with RFI and emitter scintillation that need to be addressed possibly causing some failed observations. Detection verification is stated by some players as only being acceptable using professional astronomer's pulsar software. This is misleading as none provide a yes/no answer and new pulsar search rather than recognition is their primary role. In analysis mode, *prepfold* examines the data and provides a visual display of some of the pulsar characteristic properties but offers only limited discrimination at low levels. It is only a proper scientific interpretation and confirmation of Table 1 characteristics and others, easier the larger the received pulsar amplitude, that inspires satisfactory recognition confidence. Just because a low SNR pulsar data set is recorded, it doesn't mean that it is not there. The challenge for amateurs is to apply these and other analytic processes to extract the pulsar signal from noise/RFI and not to be put off by detection statistics.

References

[1] PW. East, Getting the Best out of the PRESTO Pulsar Search & Analysis Tools., Journal of the Society of Amateur Radio Astronomers. January-February 2021.

[2] PW. East, Getting the Best out of PRESTO - Part 2 The PRESTO Period/P-Dot Search Graphic., Journal of the Society of Amateur Radio Astronomers. March-April 2021.

[3] PRESTO Home, https://www.cv.nrao.edu/~sransom/presto/

[4] SM Ransom. Searching for Pulsars with PRESTO https://www.cv.nrao.edu/~sransom/PRESTO_search_tutorial.pdf

[5] PW East, A Minimal Pulsar Detection System. Journal of the Society of Amateur Radio Astronomers. January-February 2018. p36. http://www.y1pwe.co.uk/RAProgs/MiniPulsarRx.pdf

[6] PW East. An Analytical Method of Recognizing Pulsars at Moderate SNR., Journal of the Society of Amateur Radio Astronomers. November-December 2018.

[7] PW East, A Correlation Method for Low SNR Pulsar Search and Recognition. Journal of the Society of Amateur Radio Astronomers. July-August 2019.

[8] PW East, Getting the Best Out of the Pulsar Folding Algorithm. Journal of the Society of Amateur Radio Astronomers. May-June 2021.

Appendix 1. **Improving Folded SNR**

The brown plot in Figure 4 reports the maximum peak SNR from the accumulated sections. The red plot reports the accumulated peak level at the known bin containing the pulsar signal. A method of determining this bin number is to scan the bins, in groups or singly, to find the bin whose response matches the upper part of the brown plot. This function is incorporated in the Appendix 2 MathCad program.

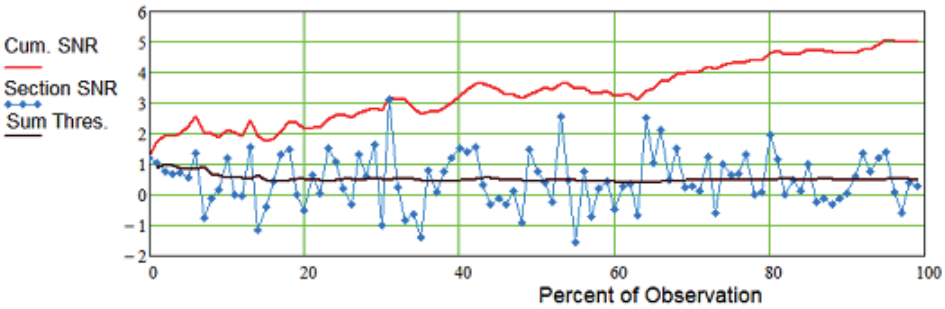

Figure A1. Accumulated Section SNR (red), block SNR (blue), SNR Threshold (black)

Inspecting Figure A1, it is evident that there are three obvious regions between sections 33 and 64 where the accumulating SNR (red) fails to increase. Close inspection of the section SNRs (blue points) reveals groups of SNRs that fall below the expected mean section SNR (black) curve. Possibly due to natural scintillation or some spurious RFI effects. In either case, it is possible to remove these sections and process the remaining sections. The result of this on the cumulative SNR plots is shown in Figure A2 after removing sections 32-35, 43-48, 55-63.

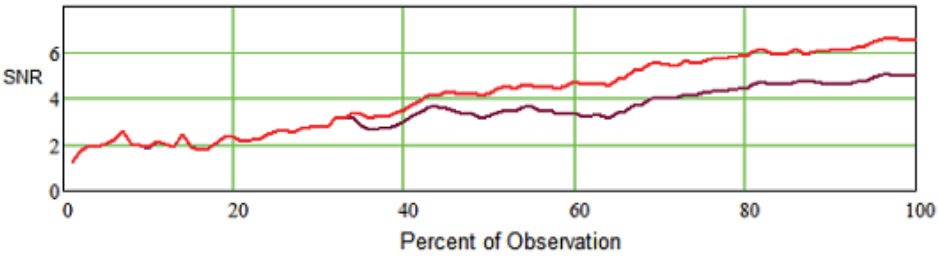

Figure A2. Accumulated Section SNR (red) with 3 Weak Sections Removed

This has had quite a significant effect in improving the final SNR showing a 30% improvement from just under 5:1 to 6.5:1. The resulting final fold is shown in Figure A3 (red) and can be compared to the original result (blue).

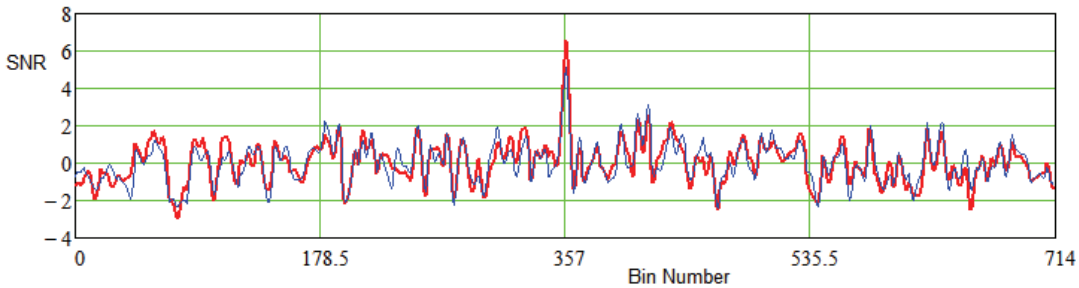

Figure A3. Final SNR (red) with 3 Weak Sections Removed Compared to All of the data SNR (blue)

It may be thought that removing data to improve the observed SNR is akin to data manipulation, but this choice is up to the user; in reflection, is this any different to RFI mitigation?

Appendix 2. MathCad Data Analysis Software

Pulsar Data Analysis and Recognition PWE May 2021

$B1 := READPRN("B311.txt")$

$B2 := READPRN("B312.txt")$ Bands 1-3 data (1ms samples)

Bands 1 and 3 de-dispersed relative to Band 2

$B3 := READPRN("B313.txt")$

$Min := 0 \quad Max := 7260000$ Number of data file samples

$i := Min .. Max - 1$ Data range

$Pt \equiv 714.4794809425$ B0329 data topocentric period (ms)

$P(p) \equiv Pt\left(1 + \frac{p}{10^6}\right)$ Pulsar Period change in ppm (ms)

$pw \equiv 6.5$ Pulsar Pulse width (ms)

$N := floor\left(\frac{Max}{Pt}\right)$ Number of periods in data file

$N = 1.016 \times 10^4$

$K := 714$ Standard Number of Fold Bins ~ 1ms time resolution

$q := 0 .. K - 1$ Fold bin range

$Nn := 100$ Number of data sections

$n := 0 .. Nn - 1$

$Bt_i := B1_i + B2_i + B3_i$ Combined de-dispersed data

$secfold_n := Stfoldpp\left(K, Pt, 0, Bt, n \cdot \frac{Max}{Nn}, \frac{n+1}{Nn} \cdot Max, pw\right)$ Data section folds

$cumsecfold^{\langle n \rangle} := \left[\sum_{x=0}^{n} \left(secfold_x\right)\right]$ Accumulating section folds

$cumsecsnr_{q,n} := snrcs\left(q, K, cumsecfold^{\langle n \rangle}\right)$ Accumulation section SNR calculation

$maxpeak_n := max\left(cumsecsnr^{\langle n \rangle}\right)$ Maximum Peak SNR in accumulated section folds

$secsnr_{q,n} := snrcs\left(q, K, secfold_n\right)$ SNR of individual section folds

$maxsnr := mx(K, Nn, cumsecsnr)$ Maximum Peak SNR in accumulated section folds + bin number

Running SNR Plot

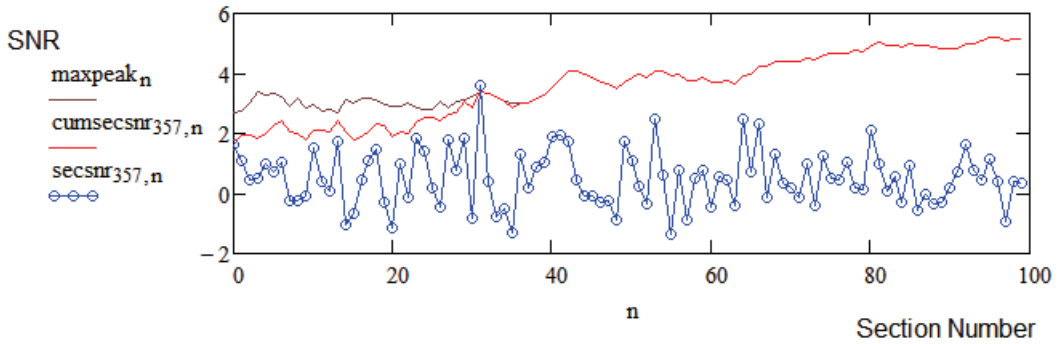

B0329 Dispersion Measure $DM := 26.7$

$$D := 4.15 \cdot DM \cdot \left[\frac{1}{(.611 - .002)^2} - \frac{1}{(.611 + .002)^2} \right]$$

Dispersion between Band1, Band 3 centres (ms) $D = 3.886$

Search Defining Equations - see Reference 6.

$$ptheory(p, N, w, P) := \frac{1}{N} \cdot \sum_{n=1}^{N} e^{-4 \cdot \ln(2) \cdot \left[\frac{p \cdot \left(1 - \frac{n}{N}\right)}{\frac{2 \cdot w \cdot 10^6}{N \cdot P}} \right]^2}$$

period search amplitude profile
peak value v period p in ppm

$$pdtheory(t, N, w, pd, P) := \frac{1}{N} \cdot \sum_{n=1}^{N} e^{-4 \cdot \ln(2) \cdot \left[\frac{t + (n-1) \cdot (n-2) \cdot \left(\frac{pd}{10^{10}}\right) \cdot \frac{P}{2}}{w} \right]^2}$$

p-dot search amplitude profile
amplitude profile v time for
p-dot value in parts/10^-10 s/s

$$distheory(d, B, w) := \frac{1}{B} \cdot \sum_{n=1}^{B} \left[e^{-4 \cdot \ln(2) \cdot \left(\frac{n}{B} \cdot d - \frac{d}{2}\right)^2} \right]$$

DM search amplitude profile
peak value v dispersion across
pulse at offset 'x'

Band Folds and frequency waterfall plot

$vV1 := Stfoldpp(K, Pt, 0, B1, Min, Max, pw)$ Band 1 609MHz band centre

$vV2 := Stfoldpp(K, Pt, 0, B2, Min, Max, pw)$ Band 2 611MHz band centre

$vV3 := Stfoldpp(K, Pt, 0, B3, Min, Max, pw)$ Band 3 613MHz band centre

$Vf_{q,0} := vV1_q$ $Vf_{q,1} := vV2_q$ $Vf_{q,2} := vV3_q \cdot .5$

SNR

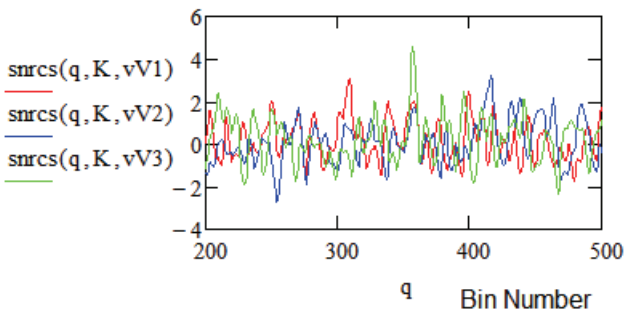

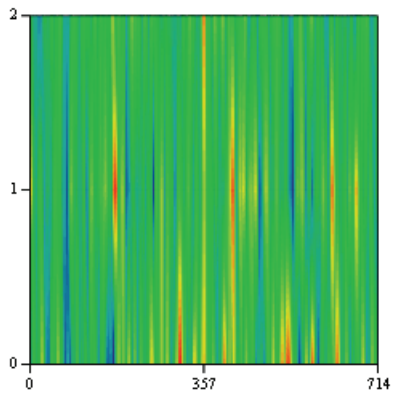

Frequency Waterfall Plot

Best profile fold

$vV := \mathrm{Stfoldpp}(K, Pt, 0, Bt, Min, Max, pw)$

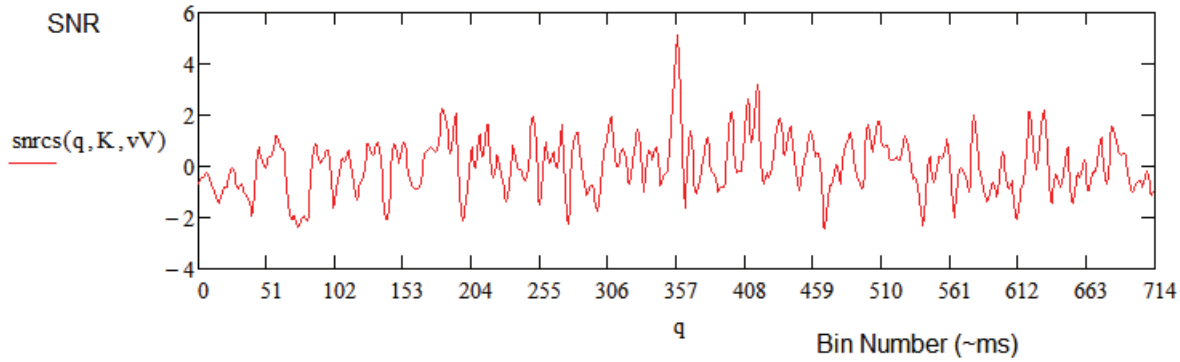

Cumulative Waterfall

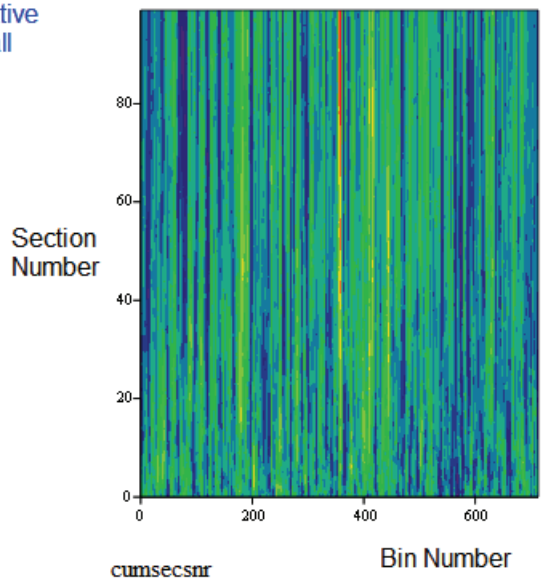

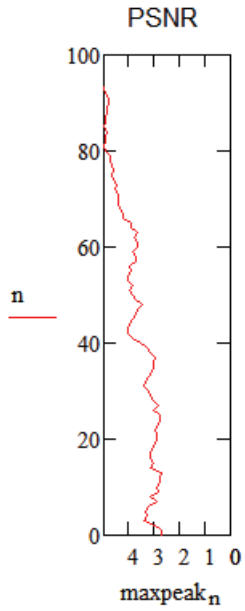

Bin Position of Peak Fold Response

$\mathrm{maxsnr}_{0,99} = 5.128$

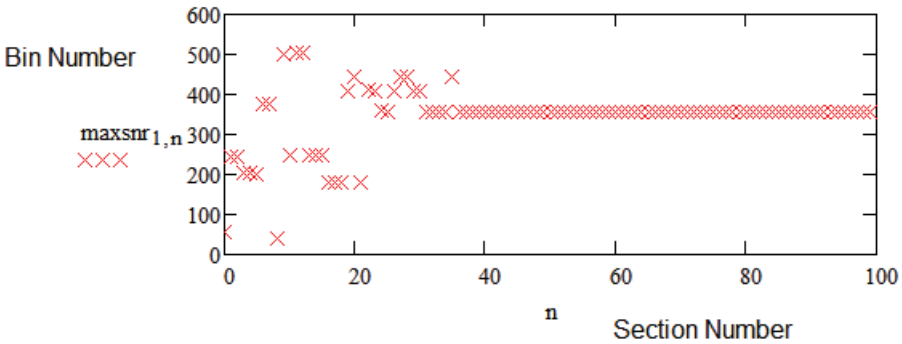

Dispersion Search

$q := 0..K-1$

$d := 0,1..24$ Dispersion search range (ms)

Dispersion band combiner

$Vd_{q,d} := vV1_{mod(q+K+4-d,K)} + vV2_{mod(q+K+0,K)} + vV3_{mod[(q+K)+d-4,K]}$

Note: range 'd' offset by +4 and -4 ms

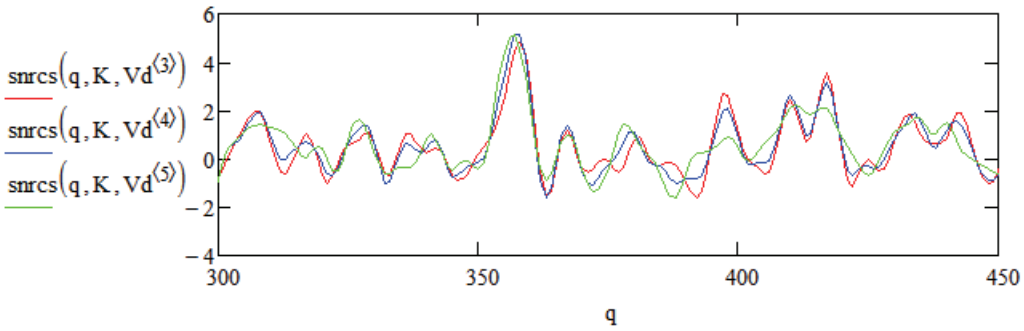

$dm_{q,d} := \left(snrcs\left(q,K,Vd^{\langle d\rangle}\right)\right)$ Actual dispersed fold SNR over search range

$DM = 26.7$

$D = 3.886$

Comparison of theoretical and practical SNR as a function of dispersion

$dd := -2,-1.9..9$ Dispersion data range (ms)

SNR

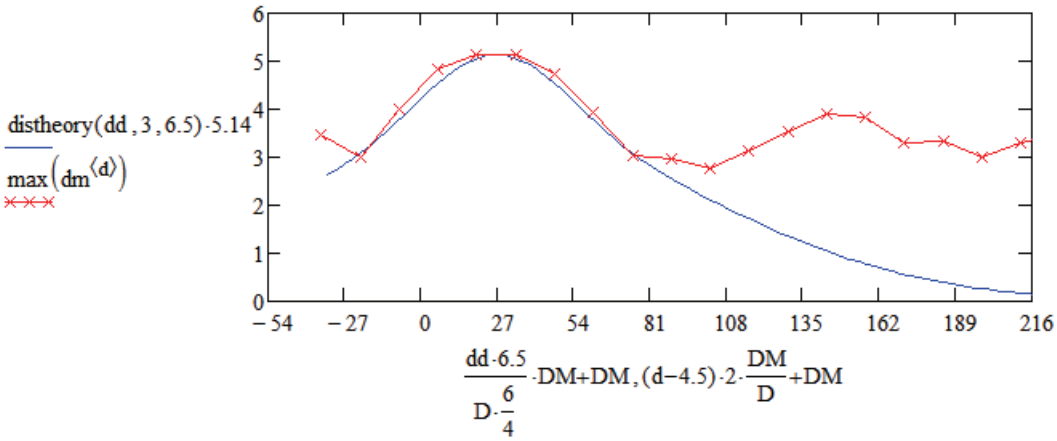

Notes:-

Data normalisation:

For the real-data plot, the x-axis should be 2(d-4)DM/D + DM as d=4, represents de-dispersed data. However, as the data is in 1ms increments and only 3 bands, the accuracy is limited. The 0.5ms offset for the real-data plot enabled an improved data symmetrical match with the theory.

For the theoretical plot, dd is indicated as a multiplier of Dp/W, where Dp is the total dispersion across the pulse (=6D/4), and W is the pulse width. When Dp/W =2 the pulse amplitude drops by one half.

Period+Pdot Search

$zz := 0..60 \qquad z := 0..60$ P-dot 'zz' and period 'z' data ranges, period in 0.5ppm and p-dot in 0.5x 10^-10 s/s, offset by 15ppm and 30x10^-10

$PPd_{z,zz} := \max[Stfoldpp[K, P[.5\cdot(z-30)], [0.5\cdot(zz-30)], Bt, Min, Max, pw]]$ 2-D PSNR calculation

$norm := \frac{maxsnr_{0,99}}{PPd_{30,30}}$ Peak SNR/amplitude normalizing factor

Comparison of theoretical and practical period search SNR over period ppm range

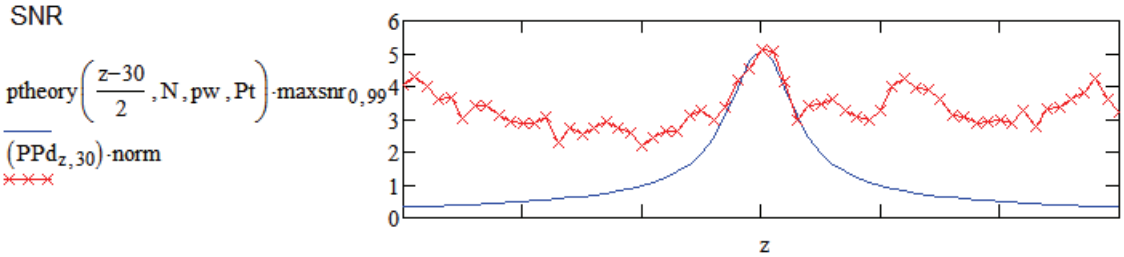

Period range: -15ppm to +15ppm

$px := 0..30$ P-dot value range to find peak

$hpk_{zz,px} := pdtheory(zz, N, pw, px, Pt)$ Search theoretical response to encompass the fold peak value over the p-dot range px and zz

$hk_{px} := \max\left(hpk^{\langle px \rangle}\right)$ Find p-dot search response peak value for each p-dot search value

Comparison of theoretical and practical p-dot search SNR over p-dot value in range range

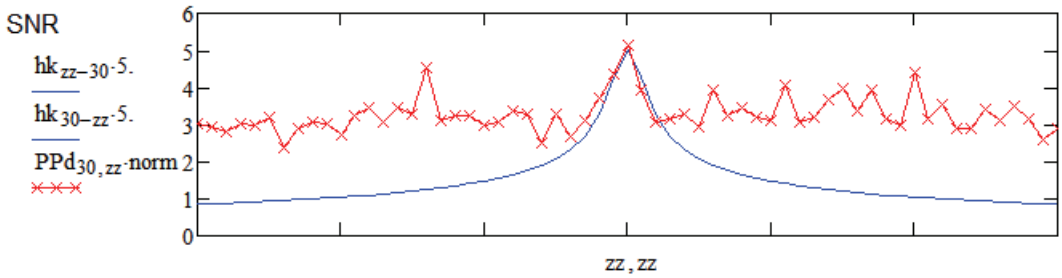

2-D period search/p-dot search plot

Pdot range: -30x 10^-10 to +30x10^-10 s/s

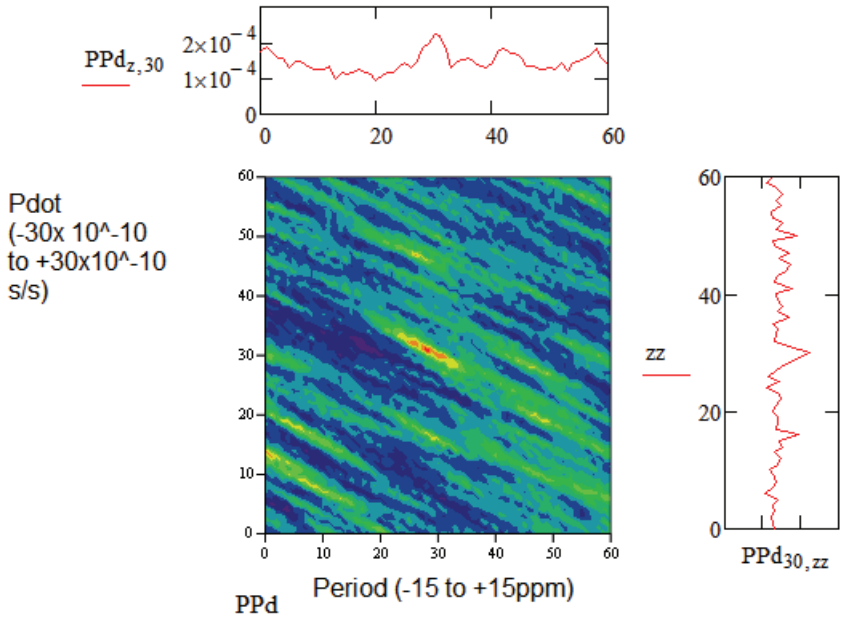

Folded data SNR calculation

```
snrcs(s, n, dat) := | mn ← 0
                    | rms ← 0
                    | mnr ← 0
                    | rmsr ← 0
                    | mx ← 0
                    | d ← floor(n/40)
                    | nx ← 0
                    | for x ∈ 0..n − 1
                    |   | mn ← mn + dat_x
                    |   | rms ← rms + (dat_x)^2
                    |   | if dat_x > mx
                    |   |   | mx ← dat_x
                    |   |   | nx ← x
                    | n1 ← floor(nx − d)
                    | n1 ← 0 if n1 < 0
                    | n2 ← floor(nx + d)
                    | n2 ← n − 1 if n2 > n − 1
                    | for x ∈ n1..n2
                    |   | mnr ← mnr + dat_x
                    |   | rmsr ← rmsr + (dat_x)^2
                    | mn ← (mn − mnr) / (n − (n2 − n1) − 1)
                    | rms ← (rms − rmsr) / (n − (n2 − n1) − 1)
                    | rms ← rms − mn^2
                    | out ← (dat_s − mn) / √rms
                    | out
```

2-D data peak/position calculation

```
mx(q, n, dat) := | for x ∈ 0..n − 1
                 |   | nx_0,n ← 0
                 |   | nx_1,n ← 0
                 | for x ∈ 0..n − 1
                 |   | for y ∈ 0..q − 1
                 |   |   if dat_y,x > nx_0,x
                 |   |     | nx_0,x ← dat_y,x
                 |   |     | nx_1,x ← y
                 |   | nx
                 | nx
```

2-D Bandwidth - matched fold algorithm for period and p-dot search

$$
\begin{aligned}
&\mathrm{Stfoldpp}(B, P, p, Dat, Min, Max, w) := \\
&\quad \text{for } fs \in 0..B-1 \\
&\qquad bdat_{fs} \leftarrow 0 \\
&\qquad bcount_{fs} \leftarrow 0 \\
&\quad \text{for } x \in Min..Max-1 \\
&\qquad P2 \leftarrow P\cdot\left(1+\frac{2\cdot x\cdot p}{1000000\cdot Max}\right) \\
&\qquad s \leftarrow \mathrm{floor}\left[\left(\frac{x}{P2}-\mathrm{floor}\left(\frac{x}{P2}\right)\right)\cdot B\right] \\
&\qquad bdat_s \leftarrow bdat_s + Dat_x \\
&\qquad bcount_s \leftarrow bcount_s + 1 \\
&\quad \text{for } b \in 0..B-1 \\
&\qquad bindat_b \leftarrow \frac{bdat_b}{bcount_b} \\
&\qquad cw_b \leftarrow .1\cdot\exp\left[-4\cdot\ln(2)\cdot\left(\frac{b-\frac{B}{2}}{\frac{w}{1.5}\cdot\frac{B}{P}}\right)^2\right] \\
&\quad fdat \leftarrow \mathrm{cfft}(bindat) \\
&\quad fdat_0 \leftarrow 0 \\
&\quad fc \leftarrow \mathrm{cfft}(cw) \\
&\quad \text{for } b \in 0..B-1 \\
&\qquad ffda_b \leftarrow fdat_b\cdot\left|\frac{fc_b}{fc_0}\right| \\
&\quad tdat \leftarrow \mathrm{icfft}(ffda) \\
&\quad \mathrm{Re}(tdat)
\end{aligned}
$$

PWE 2021

PW East July 2021

Appendix 3 SNR - Ratio or dB?

Signal-to-noise ratio is officially defined as a power ratio which is measured by a power meter and converted to a decibel (dB) measure by taking its logarithm to the base 10 and multiplying this by 10. This is fine until the signal plus noise is demodulated/detected, either by a square-law detector or the components squared and summed as for digital I/Q samples. Strictly, these outputs are now equivalent voltages so to convert this voltage ratio to dB, the logarithm of this voltage ratio should be multiplied by 20. Often in amateur radio astronomy, the x10 multiplier is used and this is OK if it is remembered that this figure now refers to the signal-to-noise power ratio at the RF input, <u>not</u> at the measurement point. To prevent this confusion, it is generally agreed that for pulsar work the SNR measure is always presented in its linear ratio form, as throughout this article.

Peter East, *pe@y1pwe.co.uk* is retired engineer from a career in radar and electronic warfare system design. He has authored a book on Microwave System Design Tools, is a member of the British Astronomical Association since the early '70s and joined SARA in 2013. He has had a lifelong interest in radio astronomy; presently active in amateur detection of pulsars using SDRs, and researching low SNR pulsar recognition. He encourages free information exchange in the amateur community and is keen to widen interest in radio astronomy generally. He maintains an active RA website at *http://www.y1pwe.co.uk*